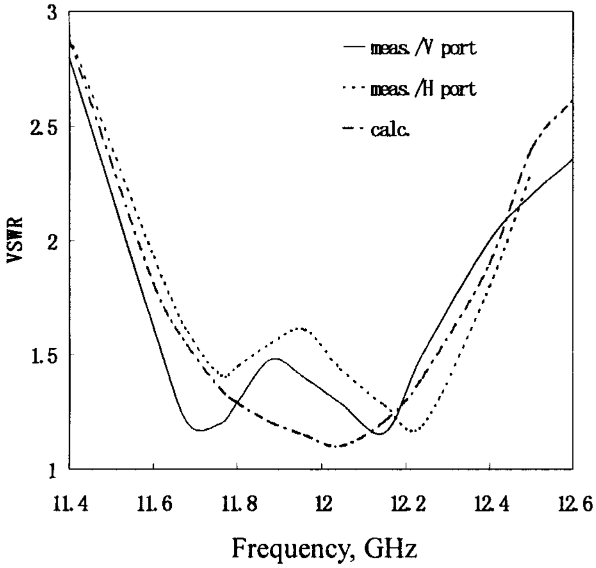

Figure 5 VSWR at two input ports

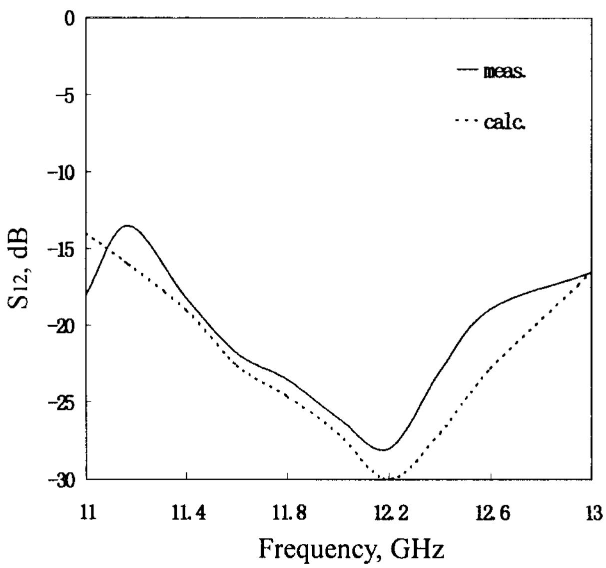

Figure 6 Isolation between two iput ports

4. CONCLUSION

A new low-cost dual-polarized array of corner-fed patches is presented. Its advantages are small size, low cost, higher isolation, lower cross polarization, etc. The radiation patterns for both co- and cross polarizations are formulated and calculated. Its S-parameters are found by using the CAD-oriented EMN method for thin microstrip antennas, which combines the cavity model, the multiport network model, and segmentation and desegmentation techniques. The theoretical results are validated by comparison with experimental results. The measured isolation of the 4×4 array is 26.5 dB at 12.0 GHz, which is obviously better than that of the classical ones.

The dual-polarized array presented in this paper can be improved further by means of corrections in the feeder width and length, corporate feed design, etc. They are promising for practical applications.

REFERENCES

1. P. Brachat and J.M. Baracco, Dual-polarization slot-coupled printed antennas fed by stripline, IEEE Trans Antennas Propagat 43 (1995), 738–742.
2. A.G. Derneryd, Microstrip Array Antenna, Proc 6th European Microwave Conference, 1976, 339–343.
3. M.J. Cryan and P.S. Hall, Integrated active antenna with simultaneous transmit-receive operation, Electron Lett 32 (1996), 286–287.
4. Y. Murakami, J. Chiba, and Y. Karasawa, Slot-coupled self-diplexing array antenna for mobile satellite communications, Proc Inst Elect Eng 143 (1996), 119–123.
5. B. Lindmark et al., Dual-polarized aperture-coupled patch multibeam antenna, IEEE AP-S Int Symp Dig, Atlanta, GA, 1998, pp. 328–331.
6. S.C. Gao and S.S. Zhong, Dual-polarized microstrip antenna array with high isolation fed by coplanar network, Microwave Opt Technol Lett 19 (1998), 214–216.
7. E.M. Cruz and J.P. Daniel, Experimental analysis of corner-fed printed square patch antennas, Electron Lett 27 (1991), 1410–1412.
8. W.F. Richards, Y.T. Lo, and D.D. Harrison, An improved theory for microstrip antennas and applications, IEEE Trans Antennas Propagat AP-29 (1981), 38–47.
9. S.S. Zhong, Microstrip antenna theory and applications, Xidian University Press, P.R. China, 1991.
10. S.C. Gao, Microstrip antenna elements and dual-polarized arrays for active integration, Ph.D. dissertation, Shanghai University, P.R. China, 1999.

CCC 0895-2477/00

PARALLEL EFFICIENT THREE-DIMENSIONAL BEAM PROPAGATION METHOD USING THE DU FORT–FRANKEL TECHNIQUE

Husain M. Masoudi[1] and John M. Arnold[2]
[1] Department of Electrical Engineering
King Fahd University of Petroleum and Minerals
Dhahran, Saudi Arabia
[2] Department of Electronics and Electrical Engineering
University of Glasgow
Glasgow, Scotland

Received 24 August 1999

ABSTRACT: *We implement the Du Fort–Frankel modified explicit finite-difference beam propagation method (MEFD) to model three-dimensional optical devices using parallel computers. Accuracy comparisons with other parallel FD–BPMs are made, and we observe that the MEFD is very accurate and efficient. The parallel implementation of MEFD shows a large run-time computer savings compared to other parallel FD–BPM algorithms.* © 2000 John Wiley & Sons, Inc. Microwave Opt Technol Lett 24: 179–182, 2000.

Key words: *beam propagation method; finite-difference analysis; modeling; numerical analysis; optical waveguide theory; partial differential equations; parallel processing implementations*

I. INTRODUCTION

As we come to the stage of integrating many optical processing elements onto one substrate, the optical circuit is becom-

Contract grant sponsor: British Council

ing large and complicated. Very efficient modeling techniques are essential in this area. The beam propagation method (BPM) is one of the methods that provide accurate and simple predictions for a variety of optical devices [1–2]. However, there are several versions of BPM, with the finite-difference BPMs being the simplest, the most flexible, and efficient [1–5]. For three-dimensional devices on the order of several thousand wavelengths in length, the problem becomes very large for conventional computers (serial) to execute efficiently [3–5]. The best way to model a large problem efficiently is to use parallel processing. However, not all algorithms are suitable for parallel processing in terms of speed up and efficiency. Those algorithms that use fewer communications between processors are said to be highly parallel, for example, the explicit finite-difference BPM and the real space BPM. In earlier work, we showed implementations and comparisons between these methods in the parallel domain [4–5]. We observed from the comparison that the parallel EFD is more efficient than the RS because it is faster per propagation step, and the two methods relatively converge using the same propagational step. Also, the EFD was found to be very efficient in analyzing 3-D devices of second-harmonic generation using second-order nonlinearities [3, 6–7]. The only disadvantage with the EFD is that it is conditionally stable, which restricts the propagational step to a very small value when the transverse mesh spacing is reduced. On the other hand, a modification to the EFD using the Du Fort–Frankel approach [8] shows two advantages over the EFD [3, 9]. The first is that the propagation step can be relaxed compared to that of the stability value of the EFD, and the second is that the total number of computations can be reduced by half by using a leapfrog arrangement. In addition, the MEFD remains explicit, and hence highly parallel. In a recent communication, we analyzed the 2-D MEFD, and compared it with the most popular FD–BPMs [10]. The only precaution with the MEFD is that it introduces a weak spurious field that is coupled to the true field. In the previous analysis, we showed some numerical solutions to reduce or eliminate these problems. In this work, we extend the MEFD to three dimension using parallel-processing implementations. In addition, a verification of the accuracy of the method is made by analyzing a 3-D rib waveguide, and the results are compared to the accuracy of the parallel EFD and the parallel RS.

II. NUMERICAL METHOD

Starting with the scalar parabolic equation for a three-dimensional field ϕ:

$$2jk_0 n_0 \frac{\partial \phi}{\partial z} = \frac{\partial^2 \phi}{\partial x^2} + \frac{\partial^2 \phi}{\partial y^2} + k_0^2(n^2 - n_0^2)\phi \qquad (1)$$

where n_0 is a reference refractive index, k_0 is the free-space wavenumber, and $n(x, y, z)$ is the refractive index, and using the central finite-difference approximations for the partial derivatives leads to the discrete EFD equation [11]:

$$\begin{aligned}\phi_{i,m}(z + \Delta z) &= \phi_{i,m}(z - \Delta z) + a_x[\phi_{i-1,m}(z) + \phi_{i+1,m}(z)] \\ &\quad + a_y[\phi_{i,m-1}(z) + \phi_{i,m+1}(z)] + b_{i,m}\phi_{i,m}(z) \qquad (2)\end{aligned}$$

where

$$\begin{aligned} b_{i,m} &= (\Delta z / jk_0 n_0)[k_0^2(n_{i,m}^2 - n_0^2) - 2/\Delta x^2 - 2/\Delta y^2] \\ a_x &= \Delta z/(jk_0 n_0 \Delta x^2) \\ a_y &= \Delta z/(jk_0 n_0 \Delta y^2). \end{aligned}$$

i and m represent the discretization of the transverse coordinates x and y, respectively, with transverse mesh sizes Δx and Δy, and Δz is the longitudinal step size. Equation (2) is stable if [11]

$$\Delta z < 2k_0 n_0 \big/ [(4/\Delta x^2) + (4/\Delta y^2) + k_0^2 |n_{i,m}^2 - n_0^2|_{\max}].$$

For accurate modeling of a typical optical device, Δx and Δy have to be kept much smaller than the optical wavelength, resulting in a very small propagation step size Δz according to the above condition. However, if the field $\phi_{i,m}(z)$ in Eq. (2) is replaced by its average value [8]

$$\phi_{i,m}(z) = [\phi_{i,m}(z + \Delta z) + \phi_{i,m}(z - \Delta z)]\big/2$$

this leads to the Du Fort–Frankel method (or the MEFD in short) [3, 8–10]:

$$\begin{aligned}\phi_{i,m}&(z + \Delta z) \\ &= c_{i,m}\phi_{i,m}(z - \Delta z) + d_{i,m}^x[\phi_{i-1,m}(z) + \phi_{i+1,m}(z)] \\ &\quad + d_{i,m}^y[\phi_{i,m-1}(z) + \phi_{i,m+1}(z)] \qquad (3)\end{aligned}$$

where

$$\begin{aligned} c_{i,m} &= (2 + b_{i,m})/(2 - b_{i,m}) \\ d_{i,m}^x &= 2a_x/(2 - b_{i,m}) \\ d_{i,m}^y &= 2a_y/(2 - b_{i,m}). \end{aligned}$$

The Du Fort–Frankel method is unconditionally stable in a uniform medium with $n^2 = n_0^2$, in contrast to the conditional stability of the standard explicit discretization (2) [10]. Examination of the EFD and the MEFD shows that the two methods require two initial fields to start the propagation. As reported earlier [10], the MEFD produces spurious fields if the two initial fields are equal or excited with other BPMs. We have suggested two numerical solutions to reduce or eliminate the spurious field. If the initial field is a guided mode, two initial fields $\phi(0)$ and $\phi(\Delta z)$ spaced by Δz can be found by multiplying $\phi(0)$ with the appropriate phase factor to obtain $\phi(\Delta z)$, assuming that the medium in the longitudinal direction does not change. The other technique is to use two equal initial fields with a very small initial step size Δz, increasing gradually to the desired Δz. Experiments with this method show that, as the initial Δz decreases, the error of the spurious field reduces.

III. RESULTS

We have implemented the three-dimensional MEFD using domain decomposition on an MIMD parallel processing machine (a 64-processor Parsytec transputer array). The implementation of the MEFD is similar to that of the EFD and the RS in [3–5]. The processor array is configured in a 2-D grid technology, and the transverse mesh points are divided into a 2-D grid of equal blocks of data. Each block of data is

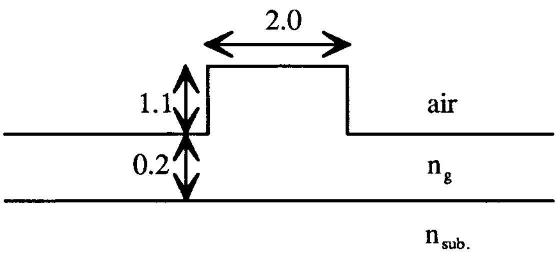

Figure 1 Rib waveguide used in the computations with $n_g = 3.44$ and $n_{sub} = 3.34$ and a wavelength of 1.55 μm

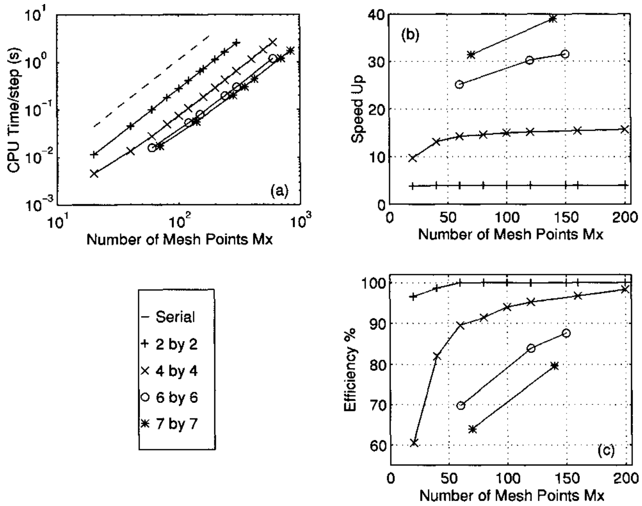

Figure 2 Speed, speed up, and efficiency of the parallel MEFD as a function of the total mesh points M_x ($M_y = M_x$). (a) Speed. (b) Speed up. (c) Percentage efficiency

assigned to one of the processors in the 2-D processor array; this arrangement ensures that the system loading is balanced. In all of the following results, the rib waveguide in Figure 1 has been used to test the MEFD. Figure 2 shows the speed, the speed up, and the efficiency in using the multiprocessor array as a function of the number of mesh points. For simplicity, the number of mesh points in the x-direction (M_x) and the y-direction (M_y) are equal. From the figure, for a fixed number of mesh points, the speed of the MEFD increases as the number of processors increases. The figure also shows that some of the implementations of the MEFD approach 100% efficiency. The serial implementation could not be continued beyond $M_x = 200$ due to the memory limit. As expected, the results in Figure 2 are similar to those of parallelizing the EFD in [4–5] because the number of operations for the two methods is close. We also expect that the implementation of the MEFD on an SIMD machine will produce a similar speed up to that of the EFD (this has not been implemented due to the unavailability of an SIMD machine). Figure 3 shows a comparison of the accuracy among the parallel EFD, the parallel RS, and the parallel MEFD as a function of Δz for different transverse mesh spacings. The results of the parallel EFD and the parallel RS are those appearing in [4–5]. The power spectral method has been used to calculate the mode indexes from the BPM fields [12]. First, the correlation function between the input and the marched field is evaluated numerically during the course of

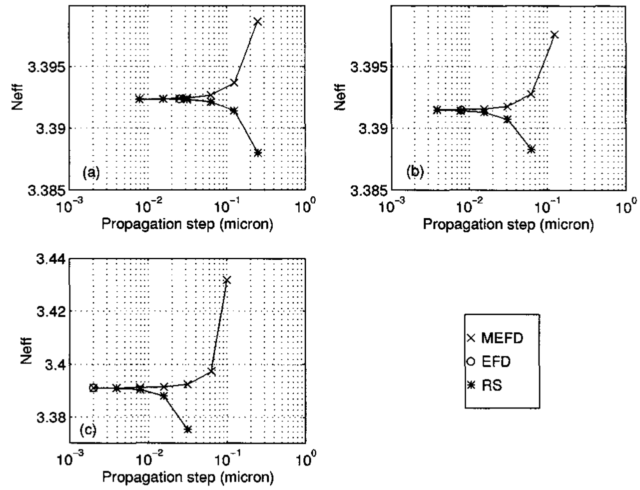

Figure 3 Convergence of the MEFD, EFD, and RS as a function of the longitudinal step size Δz. (a) $\Delta x = \Delta y = 0.1$ μm. (b) $\Delta x = \Delta y = 0.05$ μm. (c) $\Delta x = \Delta y = 0.025$ μm

propagation; then the result is multiplied with a Hanning window function and Fourier transformed. The propagation constant is computed by locating the peak of the spectrum. This figure shows the convergence of the three methods by reducing Δz, where Δz for the EFD is constrained by the stability condition of the algorithm. Comparison between the EFD and the MEFD of Figure 3(c) shows that the MEFD can use Δz about ten times larger than EFD with very little degradation in accuracy. In addition, using the leapfrog arrangement [3, 9–10], the total mesh points of the MEFD can be divided into two equal sets (even and odd), in which only one set could be used in the computation while retaining the same accuracy. This gives the MEFD a further 50% increase in the speed per propagational step over the EFD. Figure 4 shows a 3-D plot for the first guided mode of the waveguide in Figure 1 computed using the MEFD. At the end, it has to be mentioned that all of the results shown in this work were written in Fortran with a double-precision accuracy under the PARIX operating environment software.

IV. CONCLUSION

In conclusion, the modified explicit finite-difference (MEFD) BPM has been extended to three dimensions using an MIMD

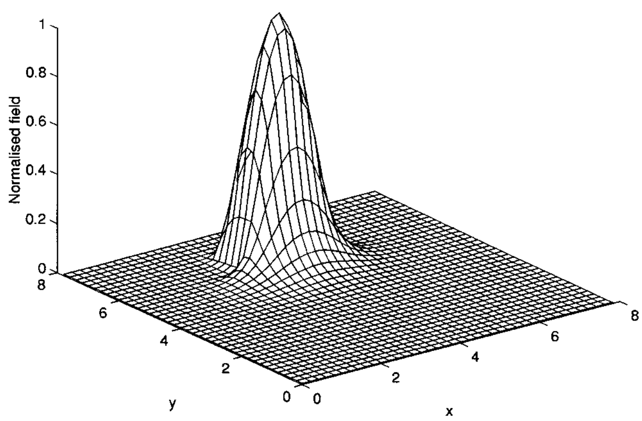

Figure 4 Three-dimensional field plot of the first guided mode of the rib waveguide of Figure 1 computed using the MEFD

parallel-processing machine. This method is very similar to the known EFD in being simple and highly parallel. A very high efficiency of parallelizing the MEFD has been recorded, due to the explicit nature of the method, which keeps the communication overhead between processors to a minimum. In addition, the accuracy of the parallel MEFD has been verified and compared with the parallel EFD and the parallel RS. Comparisons among these three methods show that the MEFD is much more efficient than both of the other techniques. Finally, the solution of the parabolic equation, discussed in this work, is common for many large major mathematical applications where the same implementations of the parallel MEFD technique could be used to speed up their execution time.

ACKNOWLEDGMENTS

Dr. Masoudi gratefully acknowledges the support of King Fahd University of Petroleum and Minerals, Dhahran, Saudi Arabia.

REFERENCES

1. D. Yevick, A guide to electric field propagation techniques for guided-wave optics, Opt Quantum Electron 26 (1994), 185–197.
2. H.J.W.M. Hoekstra, On beam propagation methods for modelling in integrated optics, Opt Quantum Electron 29 (1997), 157–171.
3. H.M. Masoudi, Parallel numerical methods for analysing optical devices with the BPM, Ph.D. dissertation, Faculty of Engineering, University of Glasgow, Scotland, 1995.
4. H.M. Masoudi and J.M. Arnold, Parallel beam propagation methods, IEEE Photon Technol Lett 6 (1994), 848–850.
5. H.M. Masoudi and J.M. Arnold, Parallel three-dimensional finite-difference beam propagation methods, Int J Numer Modeling 27 (1995), 95–107.
6. H.M. Masoudi and J.M. Arnold, Parallel beam propagation method for the analysis of second harmonic generation, IEEE Photon Technol Lett 7 (1995), 400–402.
7. H.M. Masoudi and J.M. Arnold, Modeling second-order nonlinear effects in optical waveguides using a parallel-processing beam propagation method, IEEE J Quantum Electron 31 (1995), 2107–2113.
8. E.C. Du Fort and S.P. Frankel, Stability conditions in the numerical treatment of parabolic differential equations, MTAC 7 (1953), 135–153.
9. F. Xiang and G.L. Yip, An explicit and stable finite-difference 2-D vector beam propagation method, IEEE Photon Technol Lett 6 (1994), 1248–1250.
10. H.M. Masoudi and J.M. Arnold, Spurious modes in the Du Fort–Frankel finite-difference beam propagation method, IEEE Photon Technol Lett 9 (1997), 1382–1384.
11. Y. Chung and N. Dagli, Analysis of Z-invariant and Z-variant semiconductor rib waveguides by explicit finite difference beam propagation method with nonuniform mesh configuration, IEEE J Quantum Electron 27 (1991), 2296–2305.
12. M.D. Feit and J.A. Fleck, Computation of mode eigenfunctions in graded index optical fibers by the propagating beam method, Appl Opt 19 (1980), 2240–2246.

COUPLING THROUGH A DOUBLE SLIT BETWEEN TWO PARALLEL-PLATE WAVEGUIDES

Hyo J. Eom[1] and Seunghyun Min[1]
[1] Department of Electrical Engineering
Korea Advanced Institute of Science and Technology
373-1, Kusong Dong, Yusung Gu, Taejon, Korea

Received 1 July 1999

ABSTRACT: *A solution for coupling through a double slit between two parallel-plate waveguides is obtained in analytic series form. The Fourier transform is used to express the scattered field in the spectral domain in terms of waveguide modes. The simultaneous equations for the modal coefficients are solved to obtain the transmission and reflection coefficients in simple, rigorous, and numerically efficient series. Numerical computations are performed to illustrate the coupling and directivity characteristics of a double-split coupler.* © 2000 John Wiley & Sons, Inc. Microwave Opt Technol Lett 24: 182–185, 2000.

Key words: *parallel-plate waveguides; couplers; coupling slit*

1. INTRODUCTION

Electromagnetic wave coupling between rectangular waveguides is an important subject due to its directional coupler applications. Coupling by slits between rectangular waveguides has been investigated by various approximations and numerical approaches [1–5]. The purpose of this paper is to show that an analytic, rigorous solution exists for a certain multiple-aperture directional coupler of the rectangular-waveguide type. In this paper, we examine the behavior of TE-wave coupling through a double slit between two parallel-plate waveguides. The understanding of this type of coupling behavior is, in particular, useful for the study of a practical directional coupler which has coupling elements in the common narrow wall of the rectangular waveguide. The Fourier transform technique and mode matching are used to obtain a solution in rigorous, analytic form of a rapidly convergent series which is numerically efficient.

2. FIELD REPRESENTATIONS

Consider the problem of wave coupling through a thick double slit between two metallic parallel-plate waveguides (see Fig. 1). Assume that a TE (transverse-electric-to-z-axis) wave is incident on slits from port 1, and that the $e^{-i\omega t}$ time convention is suppressed throughout. In region I ($-d_1 < x < 0$), the total E-field consists of the incident and scattered fields:

$$E_y^i(x,z) = e^{ik_{zs}z}\sin(k_{xs}x) \tag{1}$$

$$E_y^{\mathrm{I}}(x,z) = \frac{1}{2\pi}\int_{-\infty}^{\infty}\tilde{E}_y^{\mathrm{I}}(\zeta)\sin(\kappa x)e^{-i\zeta z}\,d\zeta \tag{2}$$

where $0 < s < (kd_1/\pi)$, $k = 2\pi/\lambda$, $k_{xs} = (s\pi/d_1)$, $k_{zs} = \sqrt{k^2 - k_{xs}^2}$, and $\kappa = \sqrt{k^2 - \zeta^2}$. In region II ($-d_2 < x < -d_1$, $-\alpha - a_2 < z < -\alpha + a_2$), region III ($-d_2 < x < -d_1$, $\beta - a_3 < z < \beta + a_3$), and region IV ($-d_2 < x < -d_2$), the E-fields are

$$E_y^{\mathrm{II}}(x,z) = \sum_{m=1}^{\infty}\alpha_m(x)\sin a_{2m}(z + \alpha + a_2) \tag{3}$$